Loss of intestinal core 1–derived *O*-glycans causes spontaneous colitis in mice

Jianxin Fu,[1,2] Bo Wei,[3] Tao Wen,[1] Malin E.V. Johansson,[4] Xiaowei Liu,[1] Emily Bradford,[5] Kristina A. Thomsson,[4] Samuel McGee,[1] Lilah Mansour,[6] Maomeng Tong,[3] J. Michael McDaniel,[1] Thomas J. Sferra,[6,7] Jerrold R. Turner,[5] Hong Chen,[1,7] Gunnar C. Hansson,[4] Jonathan Braun,[3] and Lijun Xia[1,2,7]

[1]Cardiovascular Biology Research Program, Oklahoma Medical Research Foundation, Oklahoma City, Oklahoma, USA. [2]Soochow University, Suzhou, Jiangsu, China. [3]Department of Pathology and Laboratory Medicine, David Geffen School of Medicine, UCLA, Los Angeles, California, USA. [4]Department of Medical Biochemistry, University of Gothenburg, Gothenburg, Sweden. [5]Department of Pathology, The University of Chicago, Chicago, Illinois, USA. [6]Department of Pediatrics and [7]Department of Biochemistry and Molecular Biology and Oklahoma Center for Medical Glycobiology, University of Oklahoma Health Sciences Center, Oklahoma City, Oklahoma, USA.

Mucin-type O-linked oligosaccharides (*O*-glycans) are primary components of the intestinal mucins that form the mucus gel layer overlying the gut epithelium. Impaired expression of intestinal *O*-glycans has been observed in patients with ulcerative colitis (UC), but its role in the etiology of this disease is unknown. Here, we report that mice with intestinal epithelial cell–specific deficiency of core 1–derived *O*-glycans, the predominant form of *O*-glycans, developed spontaneous colitis that resembled human UC, including massive myeloid infiltrates and crypt abscesses. The colitis manifested in these mice was also characterized by TNF-producing myeloid infiltrates in colon mucosa in the absence of lymphocytes, supporting an essential role for myeloid cells in colitis initiation. Furthermore, induced deletion of intestinal core 1–derived *O*-glycans caused spontaneous colitis in adult mice. These data indicate a causal role for the loss of core 1–derived *O*-glycans in colitis. Finally, we detected a biosynthetic intermediate typically exposed in the absence of core 1 *O*-glycan, Tn antigen, in the colon epithelium of a subset of UC patients. Somatic mutations in the X-linked gene that encodes core 1 β1,3-galactosyltransferase–specific chaperone 1 (C1GALT1C1, also known as Cosmc), which is essential for core 1 O-glycosylation, were found in Tn-positive epithelia. These data suggest what we believe to be a new molecular mechanism for the pathogenesis of UC.

Introduction

Ulcerative colitis (UC) is an immune-mediated disorder that results from an abnormal interaction between colonic bacteria and mucosal immune cells in a genetically susceptible host (1, 2). The mechanisms underlying this interaction remain to be defined (1, 2).

Intestinal bacterial antigens are normally shielded from encountering mucosal immune cells by the intestinal barrier, which comprises an epithelial layer and a mucus layer (3, 4). The function of the intestinal epithelial cells, limiting antigens from entering the tissues while simultaneously allowing the immune system to sample antigens in the gut, has been extensively studied (2, 5–7). The colon mucus has two layers: an outer layer, where the bacteria reside, and a bacteria-free inner layer that is firmly attached to and separates the epithelia from the commensal flora (8). The inner layer is thickest in the distal colon, where bacterial concentration is highest (3, 4). The biological significance of the inner layer, however, is poorly understood.

The colon mucus layer comprises the polymerized mucins, primarily Muc2, that are produced by goblet cells (4, 9). Mucins are glycoproteins that carry large numbers of *O*-linked oligosaccharides (*O*-glycans), which account for up to 80% of the mass of the mucin molecules and are responsible for many of the properties of mucins. *O*-glycans are synthesized post-translationally in the Golgi apparatus (10–12). All *O*-glycans are initiated with a primary structure referred to as Tn antigen (GalNAcα-*O*-Ser/Thr; Figure 1A), which is normally masked by additional glycosylation to form the main type of *O*-glycans, core 1–derived structures (12). The biosynthesis of core 1 is controlled by core 1 β1,3-galactosyltransferase (C1galt1, also known as T-synthase) (12), for which expression requires the specific molecular chaperone C1GALT1C1 in the ER (13).

Most UC patients have colitis only in the distal colon (14). Although the reasons for this regional variation are unknown, UC patients have deterioration of the mucus layer and abnormal mucin expression in the distal colon (1, 15–17). Altered intestinal O-glycosylation also occurs in patients with UC. However, the nature of the impaired O-glycosylation in UC patients is unclear (18). Whether abnormal O-glycosylation impairs the mucus inner layer and causes spontaneous colitis is unknown.

Here, we report that mice with intestinal epithelial cell–specific deficiency of core 1–derived *O*-glycans exhibited a breached inner mucus layer and developed spontaneous colitis primarily in the distal colon, which is similar to human UC. These results indicate an etiological role for impaired O-glycosylation in the pathogenesis of colitis. Notably, we discovered that Tn antigen was expressed in colon biopsy samples from a subset of UC patients and some of the Tn-expressing epithelia contained *C1GALT1C1* missense mutations. These findings support a molecular mechanism for colitis development in a subset of UC patients whereby core 1 O-glycosylation is altered through somatic mutations in *C1GALT1C1*.

Results

Mice with targeted deletion of C1galt1 in intestinal epithelial cells do not express O-glycans and develop spontaneous colitis. Core 1–derived *O*-glycans are expressed in many tissues, including the intestine. Global

Authorship note: Jianxin Fu, Bo Wei, and Tao Wen contributed equally to this work.
Conflict of interest: The authors have declared that no conflict of interest exists.
Citation for this article: *J Clin Invest.* 2011;121(4):1657–1666. doi:10.1172/JCI45538.

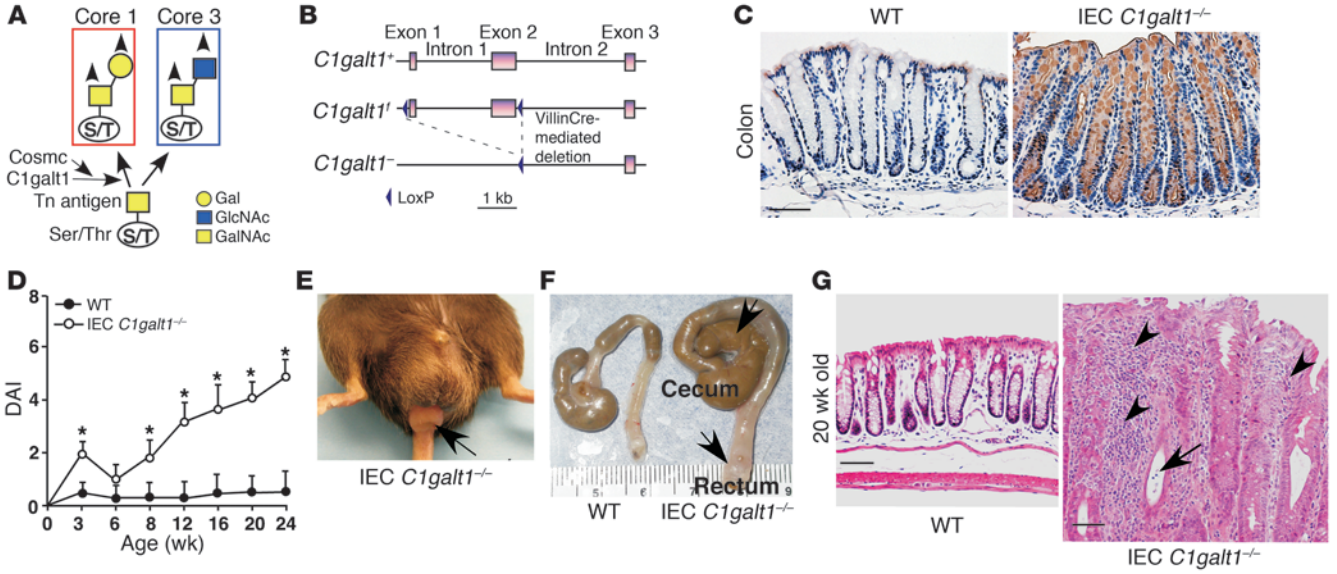

Figure 1

IEC *C1galt1*$^{-/-}$ mice develop spontaneous colitis. (**A**) Scheme for the biosynthesis of core 1 and core 3 *O*-glycans. Arrowheads indicate possible further branching to form core 1– or core 3–derived *O*-glycans, and possible fucosylation, sialylation, and sulfation. (**B**) Strategy for generating IEC *C1galt1*$^{-/-}$ mice. After crossing *C1galt1*$^{f/f}$ mice with VillinCre transgenic mice, VillinCre-mediated recombination deletes exons 1 and 2 of *C1galt1* specifically in intestinal epithelium. (**C**) Immunohistochemical staining of WT and IEC *C1galt1*$^{-/-}$ colon sections with anti-Tn. Brown indicates positive staining. (**D**) Clinical disease activity index (DAI; mean ± SD, n = 10 mice/group) of IEC *C1galt1*$^{-/-}$ mice based on diarrhea, fecal occult blood, and rectal prolapse. *$P < 0.05$. (**E**) Representative image of rectal prolapse (arrow) in an IEC *C1galt1*$^{-/-}$ mouse at 16 weeks of age. (**F**) Colonic swelling and distension (arrows) in a 20-week-old IEC *C1galt1*$^{-/-}$ mouse. (**G**) H&E-stained sections of colonic inflammation of IEC *C1galt1*$^{-/-}$ mice at 20 weeks. Arrowheads indicate inflammatory infiltrates; arrows, cryptic abscess. Scale bars: 100 μm. Data are representative of at least 3 experiments.

deficiency of mouse C1galt1 causes embryonic lethality (12). To determine the role of *O*-glycans in intestinal epithelium, we generated mice lacking C1galt1 specifically in the intestinal epithelium by crossing mice with loxP sites flanking *C1galt1* (*C1galt1*$^{f/f}$ mice) (11) with an intestinal epithelium–specific Cre-expressing transgenic line (VillinCre mice) (19). The resultant mice are referred to as intestinal epithelial cell–specific *C1galt1*$^{-/-}$ (IEC *C1galt1*$^{-/-}$) mice (Figure 1B). Antibody to Tn antigen (anti-Tn) detected Tn antigen in the IEC *C1galt1*$^{-/-}$ small and large intestinal epithelium but not in other cell types or in WT intestinal epithelium (Figure 1C), confirming the specificity of the deletion. Desialylation did not appreciably affect the intensity of anti-Tn staining (data not shown), suggesting that most exposed Tn antigens are not sialylated.

O-glycan structural analysis of the mucins purified from colon mucus demonstrated that WT mucins contained core 1–derived *O*-glycans such as fucosylated core 1, core 2 (Galβ1-3[GlcNAcβ1-6] GalNAc), and sialylated core 2 at m/z of 530, 587, and 766, respectively, but these structures were absent in IEC *C1galt1*$^{-/-}$ mucins (Supplemental Figure 1; supplemental material available online with this article; doi:10.1172/JCI45538DS1), thus verifying that deletion of *C1galt1* abolishes core 1–derived *O*-glycans. Core 3–derived *O*-glycans were detected in IEC *C1galt1*$^{-/-}$ and to a lesser extent in WT colon samples (Supplemental Figure 1), which may suggest a relative compensatory increase in core 3 O-glycosylation in the absence of core 1 O-glycosylation.

As early as 2.5 weeks after birth, IEC *C1galt1*$^{-/-}$ mice in the C57BL/6J and 129/SvImJ mixed or C57BL/6J congenic background that were raised in a specific pathogen–free facility (no detectable *Helicobacter*) began showing signs of colitis, including loose stools and fecal occult blood (Figure 1D). The disease progressed for approximately 2 weeks and then improved, suggesting a potential role for regulatory T cell function at this stage. At 8 weeks, approximately 20% of IEC *C1galt1*$^{-/-}$mice had diarrhea, and by 12 weeks, all IEC *C1galt1*$^{-/-}$ mice had diarrhea. Weight loss was evident by 8 weeks in IEC *C1galt1*$^{-/-}$ mice. Gross and microscopic examination revealed no significant abnormalities in the liver, stomach, spleen, and thymus; however, nearly 15% of IEC *C1galt1*$^{-/-}$ mice had rectal prolapse progressing over time (Figure 1E), a feature associated with murine colitis. The colons of IEC *C1galt1*$^{-/-}$ mice, especially their distal colons and rectums, had dilated and thickened walls (Figure 1F). In fact, in all mice this region was diseased and was the most severely affected; it was characterized by epithelial ulceration, inflammatory cell infiltration, goblet cell loss, epithelial hyperplasia, and, frequently, crypt microabscesses (Figure 1G). Although VillinCre deletes *C1galt1* in both small and large intestine, no significant inflammation was found in the ileum (Supplemental Figure 2). Colon has a thick, firmly attached inner and an outer loose mucus layer, whereas the small intestine only has the loose mucus layer (4). These results suggest the importance of mucus layer in maintaining the homeostasis between mucosal cells and commensal bacteria, which are at their greatest concentrations in the colon.

Adaptive immunity is not required for the initiation of colitis in IEC C1galt1$^{-/-}$ *mice.* To identify the cell type that initiates colon inflammation, we first compared various immune cell subsets in different immune compartments between WT and IEC *C1galt1*$^{-/-}$ mice. The profiles of lymphocytes and NK cells of 2.5-week-old IEC *C1galt1*$^{-/-}$ mice were similar to those of WT littermates (Supplemental Figure 3, A and B). The number of F4/80-positive macrophages was,

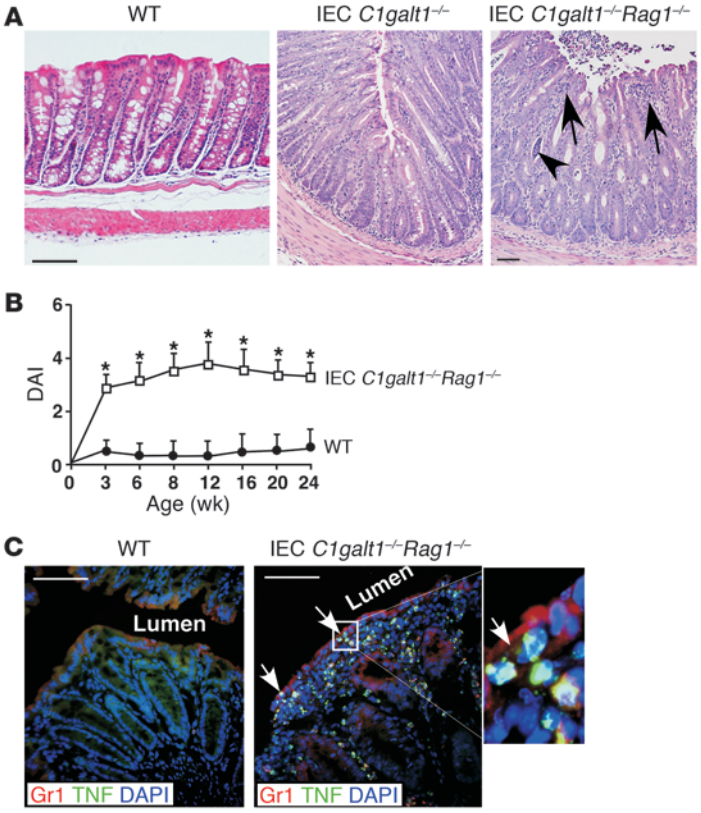

Figure 2
Adaptive immunity is not required for the initiation of colitis in IEC *C1galt1*$^{-/-}$ mice. (**A**) Representative H&E-stained colonic sections indicate similar colonic inflammation in IEC *C1galt1*$^{-/-}$ mice with and without *Rag1* deficiency at 2 weeks. (**B**) Clinical DAI (mean ± SD, $n = 10$ mice/group) of IEC *C1galt1*$^{-/-}$ mice based on diarrhea, fecal occult blood, and rectal prolapse. $^{*}P < 0.05$. (**C**) Cryosections of IEC *C1galt1*$^{-/-}$*Rag1*$^{-/-}$ colon stained with mAbs to myeloid cells (Gr1) and TNF at 3 weeks. Arrows mark infiltrates in epithelium. Inset (original magnification, ×400) highlights TNF-positive myeloid cells. Scale bars: 100 μm in **A**, 50 μm in **C**. Data are representative of at least 3 experiments.

however, significantly higher in IEC *C1galt1*$^{-/-}$ colon tissues (Supplemental Figure 3B). These results suggest that lymphocytes and NK cells are not important in colitis development in this model (2, 20). To provide definitive evidence that lymphocytes are not required for the initiation of colitis in IEC *C1galt1*$^{-/-}$ mice, we bred IEC *C1galt1*$^{-/-}$ mice with Rag1-deficient mice (*Rag1*$^{-/-}$ mice) (21), which lack lymphocytes. IEC *C1galt1*$^{-/-}$*Rag1*$^{-/-}$ mice developed colitis similar to that of their IEC *C1galt1*$^{-/-}$ littermates (Figure 2, A and B), indicating a dispensable role for lymphocytes for the colitis initiation in our model. The transient alleviation of disease severity was not observed in IEC *C1galt1*$^{-/-}$*Rag1*$^{-/-}$ mice around 6 weeks old (Figure 2B), suggesting a lack of a potential Rag-dependent T regulatory cell function in this model. At an older age (>16 weeks), the disease was less severe in IEC *C1galt1*$^{-/-}$*Rag1*$^{-/-}$ mice than in IEC *C1galt1*$^{-/-}$ littermates (Figure 1D and Figure 2B). This result suggests that lymphocytes are important for the progression of colitis at a later stage in IEC *C1galt1*$^{-/-}$ mice.

To confirm the role of myeloid cells in colitis development, we stained 3-week-old WT and IEC *C1galt1*$^{-/-}$*Rag1*$^{-/-}$ colons with antibodies to Gr1, an established marker for myeloid cells, and to TNF, a known inflammatory mediator in the pathogenesis of colitis. The 3-week-old IEC *C1galt1*$^{-/-}$*Rag1*$^{-/-}$ colon exhibited large numbers of TNF^{+}/Gr1^{+} myeloid cells (Figure 2C). Consistent with this, 2.5-week-old IEC *C1galt1*$^{-/-}$*Rag1*$^{-/-}$ sera had significantly increased levels of cytokines such as TNF, IL-6, and MCP-1 compared with WT sera (Supplemental Figure 3C), suggesting an innate immunity–driven inflammatory response.

Myeloid cells are essential for the initiation of colitis in IEC C1galt1$^{-/-}$ *mice.* To establish the role of myeloid cells in incipient disease, we first analyzed peripheral granulocytes and monocytes in IEC *C1galt1*$^{-/-}$ mice by flow cytometry. Notably, peripheral blood from IEC *C1galt1*$^{-/-}$ mice had elevated numbers of peripheral granulocytes (Ly6G^{+}CD11b^{+}) at 2 weeks and had a higher level of the inflammatory subset of monocytes (Ly-6G^{-}CD11b^{+}Ly-6C^{hi}) at 3 weeks (Figure 3A and Supplemental Figure 4). Blockage of P- and E-selectins, which inhibit myeloid cell transmigration into inflammatory sites (22), or of TNF significantly improved colitis in IEC *C1galt1*$^{-/-}$ mice as compared with IEC *C1galt1*$^{-/-}$ mice treated with control agents (Figure 3B), indicating that myeloid cells and TNF are key inflammatory initiators in our mouse model.

Further immunostaining revealed substantial infiltration of TNF-producing granulocytes and monocytes/macrophages in IEC *C1galt1*$^{-/-}$ colon tissues (2.5-week-old; Figure 3C) but not before the onset of colitis (1 week of age), suggesting that these are major cell types that sense the early microbial intrusion and initiate inflammation. We bred IEC *C1galt1*$^{-/-}$ with mice lacking Myd88, a universal adaptor protein used by most TLRs, or TLR4, which recognizes bacterial antigens, and found that neither Myd88 nor TLR4 deficiency protected IEC *C1galt1*$^{-/-}$ mice from developing colitis (Supplemental Figure 5), suggesting that TLRs are not essential for recognition of bacterial components in our mouse models.

Loss of intestinal O-glycans results in a breached inner mucus gel layer and defective mucosal integrity. Staining with Alcian blue, which recognizes acidic carbohydrates, revealed that 2.5-week-old IEC *C1galt1*$^{-/-}$ colon sections had a loss of the inner mucus gel layer (Figure 4A). Consistent with this finding, anti–Muc2–stained inner mucus layer was substantially impaired in the IEC *C1galt1*$^{-/-}$ compared with that in the WT colon. These data suggest that lack of proper O-glycosylation impairs Muc2 levels and the function of the mucus gel layer. The breached mucus integrity caused higher intestinal barrier permeability as demonstrated by the greater serum concentration of FITC-dextran in IEC *C1galt1*$^{-/-}$ mice than in WT mice after feeding with FITC-dextran (Figure 4B and ref. 23). Consequently, a significant increase in 16S bacterial ribosomal DNA (rDNA) was found in IEC *C1galt1*$^{-/-}$ as compared with WT colon (Figure 4C and ref. 23), indicating that impaired mucosal integrity increases in mucosa-associated bacteria in IEC *C1galt1*$^{-/-}$ mice.

Resident intestinal bacteria are assumed to play an important role in IBD pathogenesis (3). We found that broad-spectrum antibiotics (neomycin sulfate, metronidazole, vancomycin, and ampicillin [NMVA]) depleted gut aerobic and anaerobic bacteria (Supplemental Figure 6) and reduced colitis in IEC *C1galt1*$^{-/-}$ mice (Figure 4D), supporting a requirement for intestinal bacteria in the development of colitis in our models.

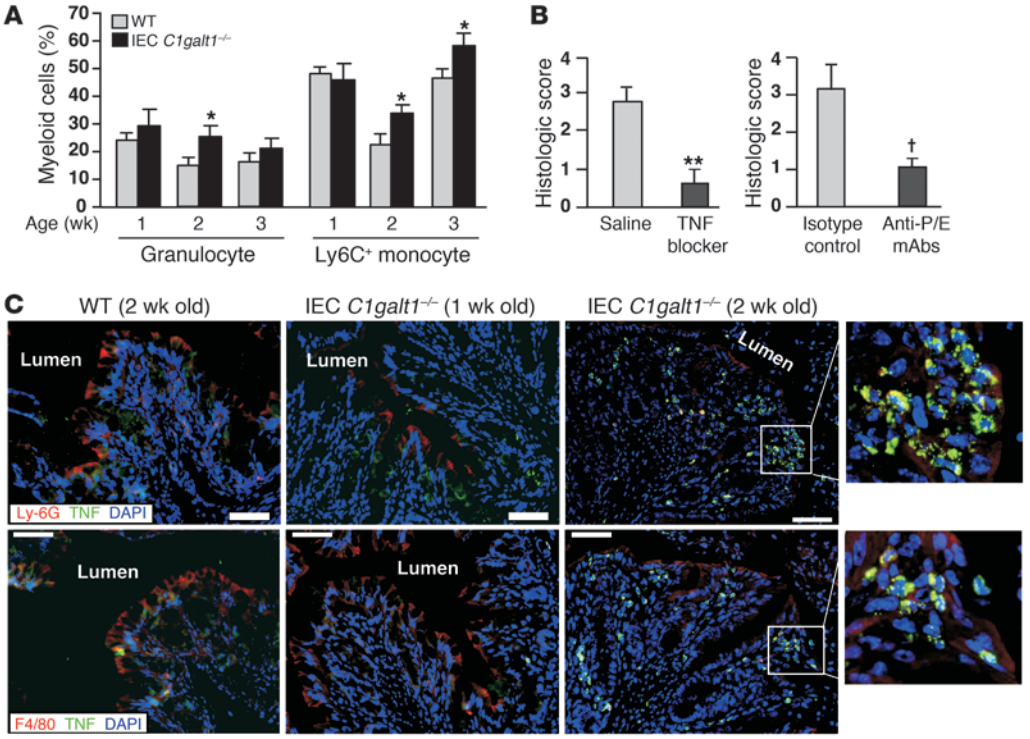

Figure 3
Innate immune cells are a critical initiator of colitis in IEC *C1galt1*$^{-/-}$ mice. (**A**) Peripheral myeloid cells analyzed by flow cytometry (mean ± SD, n = 8 mice/group). Granulocytes are defined as Ly-6G$^+$CD11b$^+$. Ly-6G$^-$CD11b$^+$ monocytes were further analyzed for Ly-6C expression. *P < 0.02. (**B**) Histologic scores of H&E-stained colon sections of 2.5-week-old IEC *C1galt1*$^{-/-}$ mice treated with etanercept (TNF blocker; saline as control, mean ± SD, n = 5 mice/group) or blocking antibodies to mouse P- and E-selectin (anti-P/E, rat IgG; isotype IgG used as controls; mean ± SD, n = 6 mice/group). **P < 0.002, †P < 0.01. (**C**) Cryosections of IEC *C1galt1*$^{-/-}$ colons at different ages stained with mAbs to granulocytes (Ly-6G), macrophages (F4/80), and TNF. Insets (original magnification, ×400) highlight TNF$^+$ granulocytes and macrophages. Scale bars: 50 μm. Data are representative of at least 3 experiments.

Inducible deficiency of O-glycans in the intestinal epithelium causes spontaneous colitis in adult mice. In IEC *C1galt1*$^{-/-}$ mice, the inactivation of *C1galt1* occurs during embryonic development, eliciting secondary host compensation, such as changes in maternal milk immunoglobulins and intestinal commensal microbiota (3). Accordingly, the colitis phenotypes of IEC *C1galt1*$^{-/-}$ neonates could reflect these secondary changes. To circumvent these potential problems and to determine whether loss of intestinal epithelial core 1–derived *O*-glycans in adult mice causes colitis, we generated mice with an inducible deficiency of intestinal epithelial *O*-glycans by crossing *C1galt1*$^{f/f}$ mice with VillinCre-ER^{T2} transgenic mice (ref. 24 and Figure 5A), in which an inert form of Cre can be activated in intestinal epithelium by administration of tamoxifen (TM). Specific and efficient inducible deletion of *O*-glycans in intestinal epithelium was achieved 2 days after 5 consecutive daily intraperitoneal injections of TM in 7-week-old *C1galt1*$^{f/f}$;VillinCre-ER^{T2} (TM-IEC *C1galt1*$^{-/-}$) mice, as indicated by anti-Tn (Figure 5B). The TM-IEC *C1galt1*$^{-/-}$ colon started to lose Alcian blue–stained glycans 5 days after TM induction, with a complete loss of the staining in the mucus layer and goblet cells by 10 days (Figure 5B). In TM-IEC *C1galt1*$^{-/-}$ colon, the thickness of the mucus gel layer was significantly reduced by 5 days and was lost by 10 days (Figure 5, B and C). Significantly, the TM-IEC *C1galt1*$^{-/-}$ colon began to show signs of colitis, such as inflammatory infiltrates, mucosal proliferation, and loss of goblet cells by 5 days after TM, and developed full-fledged colitis 10 days after TM induction, with progressive deterioration thereafter (Figure 5, B, D, and E). Like disease in IEC *C1galt1*$^{-/-}$ mice, colitis in TM-IEC *C1galt1*$^{-/-}$ mice was dependent on intestinal bacteria (Figure 5D). Thus, the loss of *O*-glycans directly caused spontaneous colitis.

Loss of intestinal O-glycans results in a defective mucus barrier. TM-IEC *C1galt1*$^{-/-}$ mice represent an ideal model to address how the lack of core 1–derived *O*-glycans causes colitis. Loss of *O*-glycans did not cause significant changes in the mRNA levels of *Muc1*, *Muc2*, *Muc3* (17), *Muc13*, and *Muc5ac* in WT and mutant colons (Supplemental Figure 7). However, the staining of Muc2, the major secreted mucus layer–forming mucin (8), and Muc3 (17), an epithelial membrane mucin, was reduced in IEC *C1galt1*$^{-/-}$ colons 5 days after TM induction (Figure 6A). Compared with WT colons, TM-IEC *C1galt1*$^{-/-}$ colons had significantly increased intestinal permeability and mucosa-associated bacteria as determined by FITC-dextran feeding and 16S-rDNA PCR, respectively, 5 days after TM induction (Figure 6, B and C). 16S rDNA in feces remained unaltered at different time points after TM, suggesting that the lack of *O*-glycans did not cause appreciable changes in the density of commensal bacteria based on PCR. FISH revealed that WT colon epithelium was covered by an intact inner layer of mucus that was devoid of bacteria. In contrast, TM-IEC *C1galt1*$^{-/-}$ epithelium had no mucus layer and directly contacted commensal bacteria (Figure 6D). These results suggest that loss of *O*-glycans causes an increased association of intestinal bacteria with TM-IEC *C1galt1*$^{-/-}$ colonic epithelia before

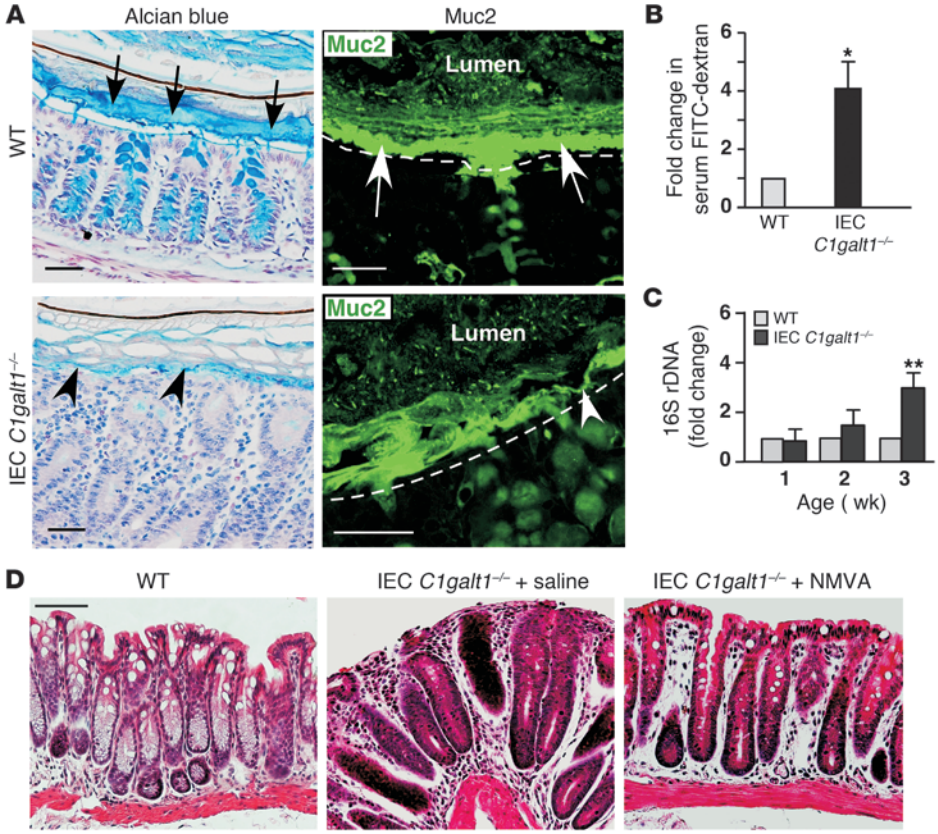

Figure 4

IEC *C1galt1*$^{-/-}$ colons have impaired mucus barrier integrity. (**A**) 2.5-week-old WT and IEC *C1galt1*$^{-/-}$ colonic tissues that were fixed with Carnoy's fixative, sectioned, and stained with Alcian blue (blue) or a FITC-labeled antibody to murine Muc2 peptide. Black arrows indicate the mucus layer. White arrows mark the inner mucus layer. Arrowheads indicate impaired mucus layer. Dashed lines mark epithelial surfaces. Scale bars: 50 μm. (**B**) Serum concentrations of the FITC-dextran of 2.5-week-old WT and IEC *C1galt1*$^{-/-}$ mice were measured 4 hours after oral administration of FITC-dextran (mean ± SD, n = 6). *P < 0.002. (**C**) Relative amount of bacterial 16S rDNA detected in colon tissues by real-time PCR using two independent sets of 16S universal primers. Data are expressed as the fold difference between WT and IEC *C1galt1*$^{-/-}$ mice (2.5 weeks old, mean ± SD, n = 6). The average 16S rDNA value of WT mice was expressed as 1. **P < 0.004. (**D**) H&E-stained representative colon sections indicate that depletion of gut microflora improves colitis in IEC *C1galt1*$^{-/-}$ mice treated with NMVA for 4 weeks starting at 8 weeks of age. Scale bars: 100 μm. Data are representative of at least 3 experiments.

full-fledged colitis occurs. Future studies of bacterial variety and density in colonic microbiota before and after colitis onset in this model are necessary to determine whether the composition of the resident bacterial population is altered.

Similar to the infiltration found in IEC *C1galt1*$^{-/-}$ mice (Figure 3C), TNF-producing myeloid cells were observed in the TM-IEC *C1galt1*$^{-/-}$ colon at the onset of colitis (5 days after TM) and became more prominent over time (Figure 6E). TNF induces tight junction molecule endocytosis and the loss of tight junction barriers (25). We observed increased internalization of the tight junction protein occludin in TM-IEC *C1galt1*$^{-/-}$ but not in the WT colonocytes 5 days after TM (Supplemental Figure 8), suggesting that the observed barrier loss at this time point is secondary to this cellular effect of TNF on epithelial tight junctions in the TM-IEC *C1galt1*$^{-/-}$ colon.

The unfolded protein response (UPR) has been genetically implicated in human IBD (26). Unlike N-linked glycosylation, which regulates protein folding in the ER, however, O-glycosylation occurs exclusively in the Golgi apparatus and is not known to regulate protein trafficking in the ER (27, 28). Nevertheless, we examined whether UPR contributed to the colitis in *O*-glycan–deficient mouse model. Our results demonstrated that TM-IEC *C1galt1*$^{-/-}$ colon epithelium did not have significant accumulation of the non–O-glycosylated Muc2 precursor in the ER (Supplemental Figure 9A). RT-PCR did not detect a spliced form of XBP-1, which is the activated form of the ER stress response transcription factor (29), in the inflamed TM-IEC *C1galt1*$^{-/-}$ colon 15 days after TM (Supplemental Figure 9B). These results indicate that an abnormal O-glycosylation–related UPR response does not occur, or at least is of such small scale that it does not induce a detectable biologic response in our model.

Colon epithelial cells from patients with UC express Tn antigen, and a subset has mutated C1GALT1C1. To investigate the clinical relevance of our *O*-glycan–deficient colitis mouse models, we stained archived paraffin-embedded colon biopsy samples from UC patients with anti-Tn. Epithelia in 8 of the 46 UC patients were Tn positive (Figure 7, A and B), whereas all 16 non-IBD samples were negative. Approximately 30% of the UC biopsy colon tissue paraffin blocks for the Tn antigen staining contained little epithelium as a result of severe inflammation/ulceration; therefore, this rate of Tn detection may be an underestimate. Tn-positive and -negative crypts often occurred within a single colon section, suggesting a clonal abnormality of O-glycosylation. Defective core 1 or core 3 O-glycosylation could lead to the exposure of Tn (12, 23). Immunohistochemical staining demonstrated that the expression of core 3 β1,3-*N*-acetylglucosaminyltransferase in UC colons was comparable to that in normal control colons (Supplemental Figure 10), suggesting defects in pathways controlling the core 1 O-glycosylation. Recently, somatic mutations in X-linked *C1GALT1C1*, which is essential for core 1 O-glycosylation (Figure 1A), were reported (30, 31). We identified 4 missense mutations in the coding sequence of *C1GALT1C1* from genomic DNA extracted from Tn-positive epithelia (Supplemental Figure 11, A–C). Sequencing of PCR products amplified from independently collected Tn-positive crypts from the same patient produced the same result, indicating that the mutations were not artifacts. Site-directed mutagenesis analysis indicated that these mutations resulted in impaired function of C1GALT1C1 (Supplemental Fig-

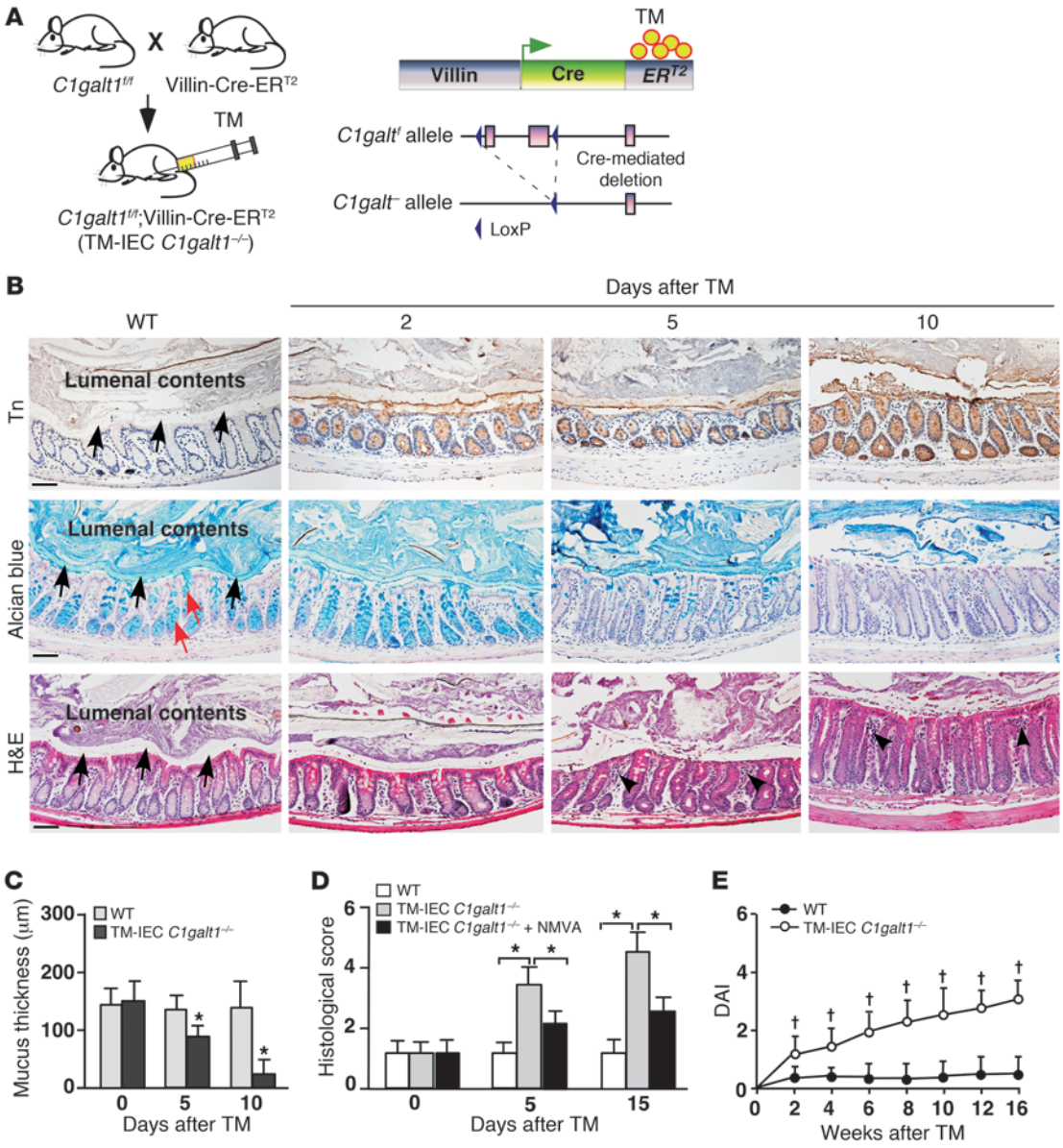

Figure 5

Inducible deletion of intestinal core 1–derived *O*-glycans causes spontaneous colitis in adult mice. (**A**) Schematic diagram of inducible intestinal epithelial cell–specific deletion of *C1galt1*. (**B**) Representative images of WT and TM-IEC *C1galt1*$^{-/-}$ colon sections at different time points after TM induction stained with an anti-Tn (brown indicates positive reaction), Alcian blue, or H&E. Black arrows indicate mucus layer or space. Red arrows indicate goblet cells. Arrowheads indicate inflammatory infiltrates. Scale bars: 200 μm. Data are representative of at least 3 experiments. (**C**) Estimation of mucus layer thickness on H&E-stained sections (mean ± SD, n = 8/group). (**D**) Histological scores of colon inflammation in TM-IEC *C1galt1*$^{-/-}$ mice with and without antibiotic treatment (NMVA) (mean ± SD, n = 10/group). (**E**) Clinical DAI (mean ± SD, n = 10 mice/group) of TM-IEC *C1galt1*$^{-/-}$ mice based on diarrhea, fecal occult blood, and rectal prolapse. *P < 0.01, †P < 0.05.

ure 11, D–F). Although large-scale high-throughput genetic analyses with sufficient power are necessary to make definitive conclusions, the observations suggest that loss-of-function mutations in *C1GALT1C1* contribute to aberrant O-glycosylation in some UC patients (Figure 7 and Supplemental Figure 11).

Discussion

Our results demonstrate that loss of intestinal *O*-glycans causes reduced levels of mucins; a breached colon mucus inner barrier, leading to increased interaction of intestinal bacteria with epithelia; and subsequently spontaneous colitis in mice (Figure 7C). This study highlights the important contribution of *O*-glycans, a primary component of mouse colon mucus, to intestinal barrier function and to the pathogenesis of UC.

Mucin synthesis and secretion decrease in active UC (15, 32, 33). The relevance of Muc2 and its *O*-glycan decoration is validated by colitis susceptibility of mice bearing genetic deficiencies in these traits (23, 34, 35). Mechanistically, their contribution to colitis sus-

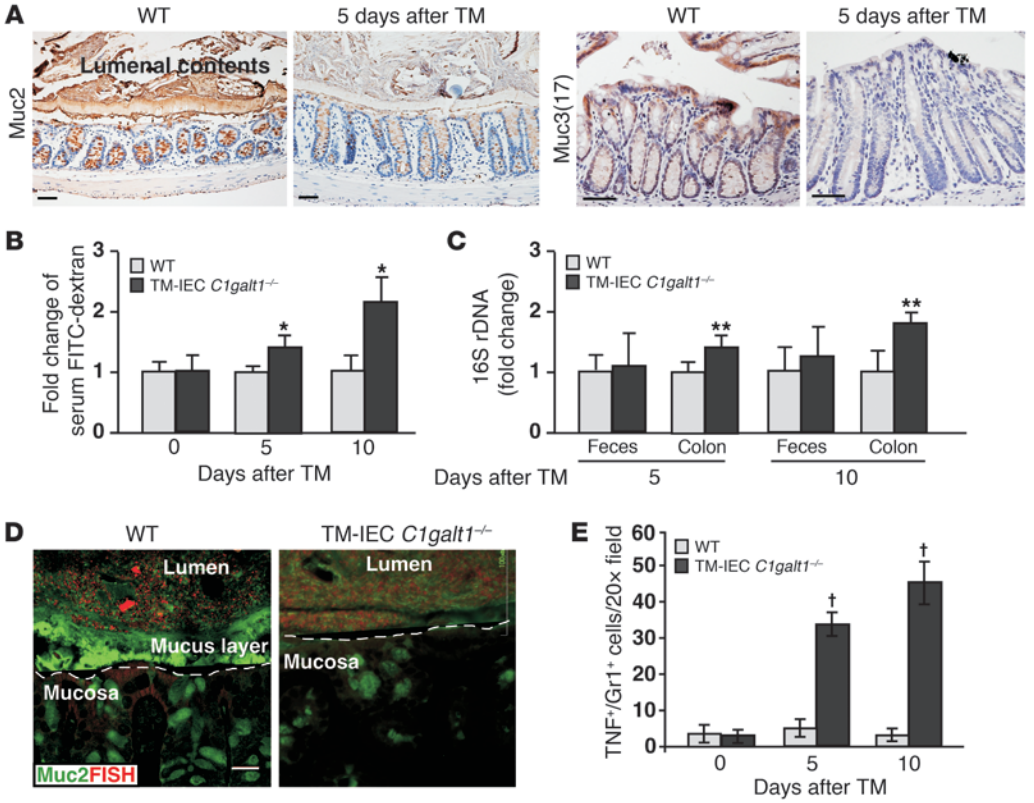

Figure 6

Absence of core 1–derived *O*-glycans impairs the levels of intestinal mucins and the integrity of intestinal barrier function. (**A**) Representative images of immunohistochemical staining (brown) with O-glycosylation–independent antibodies to different mucins in colon sections of WT and TM-IEC *C1galt1*$^{-/-}$ mice 5 days after TM. Scale bars: 100 μm. (**B**) Serum concentrations of FITC-dextran were measured 4 hours after oral administration to WT and TM-IEC *C1galt1*$^{-/-}$ mice at different time points after TM induction (mean ± SD, $n = 6$). *$P < 0.008$. (**C**) Relative amount of bacterial 16S rDNA detected by real-time PCR using two independent sets of 16S universal primers. Data are expressed as the fold difference between WT and TM-IEC *C1galt1*$^{-/-}$ mice (mean ± SD, $n = 6$). The average 16S rDNA value of WT mice was expressed as 1. **$P < 0.02$. (**D**) Colon sections of 7-week-old mice 10 days after TM induction were probed with an Alexa Fluor 555–conjugated general bacterial 16S rDNA probe for FISH (red) and costained with a FITC-labeled glycosylation-independent polyclonal antibody to Muc2 (green). Dashed lines mark epithelial surfaces. Scale bar: 20 μm. (**E**) Quantification of immunofluorescence images of 7-week-old WT and TM-IEC *C1galt1*$^{-/-}$ colon sections stained with mAbs to myeloid cells (Gr1) and TNF (mean ± SD, $n = 5$). †$P < 0.001$.

ceptibility is due at least in part to the crucial role of these structures as physical barriers to microbial intrusion, and by providing selective glycans for cognate receptors specific to restricted microbial phylotype (36–38). Few changes in mucin gene expression or polymorphisms have, however, been detected in IBD, except for the changes found in *Muc3A* (2, 39). Therefore, the cause of the abnormal mucin expression in UC remains to be defined. The IBD-associated variants of *XBP1* and *ATG16L1*, which are involved in either ER stress response or autophagocytosis, may cause secondary mucin dysfunction (26, 40). However, the causes of abnormal mucin expression and whether these alterations are causative in human UC are largely unknown. Our data indicate that *O*-glycans are essential for the expression of both secreted and membrane-associated mucins and for the integrity of the mucus layers, thus underscoring the importance of altered O-glycosylation as a causal factor in the pathogenesis of colitis. Loss of *O*-glycans may impair the expression and function of many intestinal mucins, thereby causing more profound defects in intestinal barrier function than an abnormality caused by the deficiency of an individual mucin. Indeed, compared with Muc2-deficient mice, which develop colitis only in a 129/Sv background (34), *O*-glycan–deficient mice develop more severe spontaneous colitis on either C57BL/6 and 129SV mixed or C57BL/6 congenic background.

The nature of the impaired O-glycosylation in patients with UC is unclear (18). Our studies provide the first demonstration to our knowledge that some UC colons express Tn antigen, underscoring the clinical relevance of the *O*-glycan–deficient colitis models. Significantly, our pilot study identified missense somatic mutations in *C1GALT1C1* in Tn-positive epithelial cells from UC patients. Mutations in *C1GALT1C1* are reported in patients with several diseases, including colorectal tumor cells that express Tn antigens (30, 31). These promising results suggest that altered O-glycosylation causes impaired mucus barrier function in a subset of UC patients and may serve as an etiological factor for UC. Notably, only one of the genes regulating glycosylation has been identified as relevant to known IBD loci (2, 41). Glycosylation pathways are, however, complex (42), such as the indirect regulation of C1galt1 activity by C1GALT1C1. More-focused genetic studies will be needed to determine whether mutations in genes controlling O-glycosylation are commonly associated with UC.

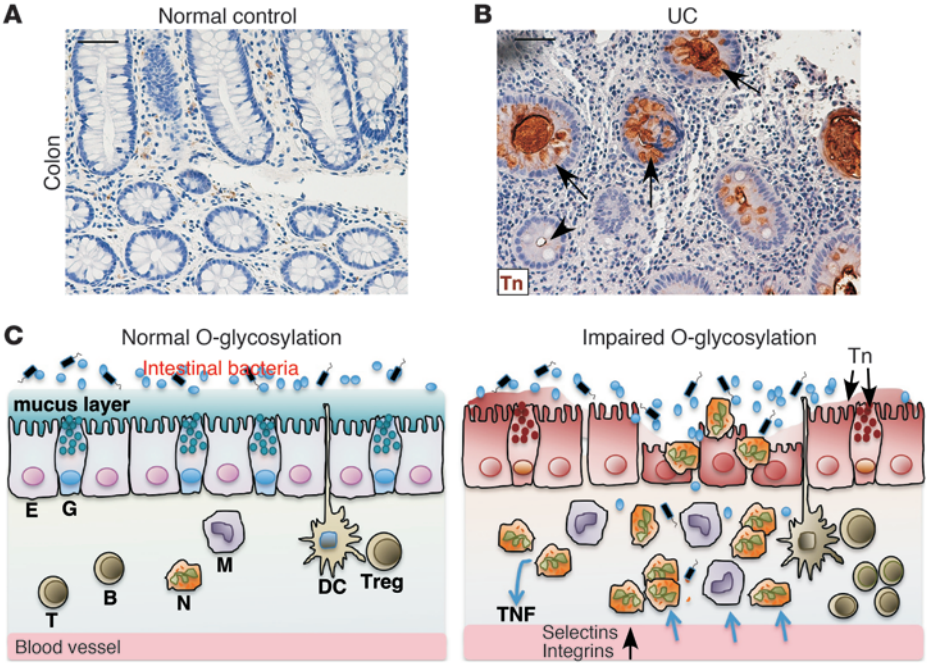

Figure 7
Colon epithelium of a subset of UC patients expresses Tn antigen. Representative immunohistochemical staining of colon biopsy samples from a normal control (**A**) and UC patient (**B**). Arrows indicate Tn-positive crypts. Arrowhead marks a Tn-negative crypt. Scale bars: 50 μm. (**C**) Model illustrating that loss of intestinal core 1–derived *O*-glycans results in an impaired mucus barrier, allowing intestinal microflora to interact abnormally with the epithelium and mucosal immune cells, which causes myeloid cell–initiated colitis that is eventually amplified and/or diversified by other innate cells and lymphocytes. E, epithelial cell; G, goblet cell; N, neutrophil; M, monocyte/macrophage; B, B cell; T, T cell.

Activation and recruitment of myeloid cells in colon mucosa are hallmarks of active UC and are associated with epithelial injury and clinical disease activity (1). However, the significance of myeloid cells in the initiation of colitis and in disease progression remains unclear. Our data indicate that myeloid cells are among the major early responders to bacterial intrusion when the mucus barrier is breached and contribute significantly to tissue damage in the *C1galt1*$^{-/-}$ colon. In general, microbial recognition is achieved through pattern recognition receptors, such as TLR and Nod-like receptors (NLRs) (1, 2, 43). The activation of myeloid cells in our models is Myd88 independent, which is similar to that in T-bet–deficient mice that exhibit colitis in the background of Rag1 deficiency (44), although, unlike in T-bet–deficient mice, spontaneous colitis in *C1galt1*$^{-/-}$ mice is not dependent on the Rag1 deficiency. The underlying mechanism of colitis susceptibility in T-bet–deficient mice includes an enteric dysbiosis resulting from their host genetic deficiency in mucosal defense, with resultant recruitment and activation of proinflammatory myeloid cells. This is different from the mechanism in *C1galt1*$^{-/-}$ mice. In *C1galt1*$^{-/-}$ mice, increased association of intestinal bacteria with colonic epithelia may result from impaired ability of the *O*-glycan–dependent mucus barrier to impede nonspecific bacterial invasion. Recent work has demonstrated that some symbiotic bacteria have developed *O*-glycan sensing and degradation pathways (45). Based on this, it can be anticipated that the changes in the *O*-glycans will alter the composition of the gut microbiota. The ability of bacteria to penetrate the mucus barrier may also contribute to the pathogenesis of colitis in our models. Nevertheless, in both models, Myd88 independence is a surprising feature, suggesting that the relevant microbial sensing in this setting of innate inflammation predominates with Myd88-independent TLR, NLR, or other families of pathogen-associated molecular products (1, 43).

With respect to modeling UC, the *C1galt1*$^{-/-}$ mouse has two additional features of note. First, unlike the existing mouse colitis models (20, 46), *C1galt1*$^{-/-}$ mice are unique in developing disease of the rectum and distal colon, a feature of human UC. Second, *C1galt1*$^{-/-}$ mice genetically confer the intestinal core 1–derived *O*-glycan deficiency observed in human UC. Therefore, *C1galt1*$^{-/-}$ mice provide evidence for a causal role of the core 1–derived *O*-glycan abnormality in UC, and can be used as a valuable model to study its pathogenesis and therapeutic strategies.

Methods

Details regarding *O*-glycan structural analysis, detection of expression of mucin genes and XBP1 by RT-PCR, detection of non–O-glycosylated Muc2 precursor in the ER, anti-C3GnT staining, and *C1GALT1C1* mutation analysis are provided in Supplemental Methods.

Mice. IEC *C1galt1*$^{-/-}$ mice and TM-IEC *C1galt1*$^{-/-}$ mice were generated by breeding *C1galt1*$^{f/f}$ mice with VillinCre transgenic mice (Tg[Vil-cre]997Gum; Jackson Laboratory) and VillinCre-ER^{T2} transgenic mice (provided by Sylvie Robine, CNRS–Institut Curie, Paris, France, and Robert Coffey, Vanderbilt University, Nashville, Tennessee, USA) (11, 19, 24, 47), respectively. To induce a postnatal deficiency in intestinal *O*-glycans, 6- to 8-week-old TM-IEC *C1galt1*$^{-/-}$ mice were injected intraperitoneally with 1 mg TM (MP Biomedicals) in an ethanol/sunflower seed oil mixture (1:9 [v/v]) for 5 consecutive days. *Rag1*$^{-/-}$ mice (Jackson Laboratory), *Tlr4*$^{-/-}$ mice, and *Myd88*$^{-/-}$ mice (originally developed by Shizuo Akira, Osaka University, Osaka, Japan) (48) were crossed to IEC *C1galt1*$^{-/-}$ mice to establish mice with combined gene deficiencies. The animal studies were conducted with protocols that had been approved by the Institutional Animal Care and Use Committee of the Oklahoma Medical Research Foundation and UCLA. Mice were raised in a specific pathogen–free barrier facility and genotyped routinely by PCR assay on genomic DNA isolated from tail clips. The primers used for genotyping include Flox1: 5′-TGACAGCCAGGAATGGAACTTG-3′ and Flox2: 5′-GCCTCTTCTCGCAACAAAATACTC-3′; CRE1: 5′-AGGTGTAGAGAAGGCACTTAGC-3′ and CRE2: 5′-CTAATCGCCATCTTCCAGCAGG-3′. Sex- and age-matched littermates were used as controls in all experiments. Unless specified, all mice were on the C57BL/6J congenic background.

Histology. For histology, tissues were freshly harvested from mice and fixed with 10% neutral buffered formalin or in Carnoy's fixative (60% meth-

anol, 30% chloroform, and 10% acetic acid) prior to paraffin embedding. Paraffin-embedded sections (5 μm) were stained with H&E. The pictures were obtained with an Eclipse E1000 microscope (Nikon). Histologic severity of colitis was assessed in a blinded fashion (23).

Evaluation of clinical activity of colitis. Mice were weighed biweekly and scored for colitis-associated symptoms, including stool consistency (0, normal; 2, loose stools; 4, diarrhea), presence of fecal blood (occult fecal blood: 0, negative; 2, positive), and rectal prolapse (0, normal; 2, present sometimes; 4, present always) (23).

Immunohistochemical and immunofluorescence staining. For Tn antigen staining, deparaffinized sections were incubated with or without 0.5 U/ml sialidase from *Arthrobacter ureafaciens* (Roche) at 37°C for 3 hours. Sections were incubated for 30 minutes with biotinylated anti-Tn (mouse IgM, provided by Tongzhong Ju and Richard Cummings, Emory University, Atlanta, Georgia, USA) or with isotype-matched control mouse IgM. Bound antibodies were detected with horseradish peroxidase–conjugated streptavidin (Vector Laboratories) (11, 23).

For immunohistochemical detection of Muc2 and Muc3, deparaffinized sections were boiled for 20 minutes in 0.01 M citrate buffer at pH 6.0 for epitope retrieval. The sections were then blocked for 20 minutes using a protein blocking kit (Dako). Endogenous avidin-binding proteins were blocked using avidin/biotin blocking reagents (Vector Laboratories). Sections were incubated overnight at 4°C with rabbit anti-Muc2 (1:200 dilution; Santa Cruz Biotechnology Inc.; epitope corresponding to amino acids 4,880–5,179, which maps to the C-terminus of mucin 2 of human origin), rabbit anti–mouse Muc3(17)-S2, which is glycosylation independent (raised against the peptide KYTPGFENTLDTVVKNLETKIKNAT), or control IgG. The sections were subsequently incubated with biotinylated anti-rabbit (Vector Laboratories) for 45 minutes, followed by a 20-minute incubation with 0.6% H_2O_2 in methanol to inhibit endogenous peroxidase activity. The sections were finally incubated with horseradish peroxidase–streptavidin (Vector Laboratories) for 30 minutes and developed with a diaminobenzidine substrate and counterstained with hematoxylin.

For the detection of infiltrated inflammatory cells, distal colons were dissected from mice and fixed in 4% paraformaldehyde at 4°C overnight, followed by cryoprotection in 20% sucrose, and then embedded in a mixture of OCT compound (Sakura Finetek) and tissue freezing medium (Electron Microscopy Sciences). Cryosections (20 μm thick) were incubated with rat mAb against murine Ly6G (5 μg/ml, clone 1A8; BD) or rat mAb against murine F4/80 (5 μg/ml, clone C1:A3-1; AbD Serotec) combined with rabbit anti–mouse TNF (polyclonal; BD) overnight at 4°C, developed with phycoerythrin-labeled goat anti–rabbit IgG (1:50; Jackson ImmunoResearch Laboratories Inc.) and Alexa Fluor 488–conjugated donkey anti–rat IgG (1:100; Invitrogen), and mounted with ProLong Gold mounting medium with DAPI (Invitrogen). Specimens were analyzed by epifluorescence imaging using a Nikon C1 confocal laser-scanning unit equipped with a 3-laser launcher mounted on an Eclipse TE200-U inverted microscope. Species-specific, isotype control antibodies were used for negative controls. For each section, 5 different high-powered microscopic fields (×20) were chosen randomly to count the TNF^+, $Ly6G^+$, and $TNF^+/Ly6G^+$ cells. DAPI-positive areas were quantified as pixels per high-powered microscopic field (×20) using Photoshop (Adobe). The cell numbers were normalized to DAPI staining.

Commensal microflora depletion. To deplete the commensal microflora in the gut, 3-week-old mice were treated with ampicillin (1 g/l), vancomycin (500 mg/l), neomycin sulfate (1 g/l) and metronidazole (1 g/l) in drinking water (49). All antibiotics were purchased from MP Biochemicals, except metronidazole (Sigma-Aldrich).

Intestinal barrier integrity. Intestinal barrier integrity was measured as described previously (23). In brief, IEC *C1galt1*$^{-/-}$ mice, TM-IEC *C1galt1*$^{-/-}$ mice, and their controls were fed 200 μl of FITC-dextran at 600 mg/kg body weight (molecular weight, 4 kDa; Sigma-Aldrich) by gavage. Blood was collected 4 hours later by retro-orbital bleeding. The serum concentration of the FITC-dextran (excitation, 490 nm; emission, 530 nm) was determined using an Infinite M200 fluorometer (Tecan). Serially diluted FITC-dextran was used to generate a standard curve. Animals were sacrificed immediately after bleeding, and intestinal cryosections were prepared for fluorescence microscopy.

Bacterial translocation. Bacterial translocation in IEC *C1galt1*$^{-/-}$ mice was evaluated with real-time PCR (23). Two sets of universal primers specific for the conserved regions of the bacterial 16S rDNA gene were used. These included 16S1 (forward, 5′-CCATGAAGTCGGAATCGCTAG-3′; reverse, 5′-ACTCCCATGGTGTGACGG-3′) and 16S2 (forward, 5′-TCCTACGGGAGGCAGCAGT-3′; reverse, 5′-GGACTACCAGGGTATCTAATCCTGTT-3′). DNA extracted from colonic tissues and colonic fecal materials was used as a template. Colonic tissues were washed carefully before extraction of DNA to remove residual feces. For the quantification of 16S rDNA in colonic tissues, a pair of primers specific to the mouse *Selp* gene (forward, 5′-ATGATTAGCAAATTCTAGCTCCTGTTT-3′; reverse, 5′-TAGGTCTCTTAGGATCTCCCTTCAAT-3′) was used in a separate reaction as the endogenous control to normalize the DNA loading between samples. For the quantification of fecal bacterial 16S rDNA, DNA from each mouse fecal sample was quantified, and 25 ng DNA was used as a template in each PCR reaction. Real-time PCR was performed on an ABI Prism 7000 spectrofluorometric thermal cycler (Applied Biosystems) using SYBR green as a double-stranded DNA–specific binding dye. The relative amount of 16S rDNA in each sample was estimated using the ΔΔCt method (23). Each sample was assayed in duplicate.

FISH. FISH was performed as described previously (8). Briefly, colon sections fixed with Carnoy's fixative were incubated with 250 μg Alexa Fluor 555–conjugated EUB (5′-GCTGCCTCCCGTAGGAGT-3′; bp 337–354 in bacteria EU622773) in 50 μl hybridization buffer (20 mM Tris-HCl, pH 7.4; 0.9 M NaCl; 0.1% SDS) at 50°C overnight. The sections were rinsed in wash buffer (20 mM Tris-HCl, pH 7.4; 0.9 M NaCl) and washed at 50°C for 15 minutes. Co-immunostaining with glycosylation-independent anti-MUC2 (C3) (8) was performed at 4°C without antigen retrieval to preserve the in situ hybridization, and sections were mounted in ProLong Gold antifade (Invitrogen). Pictures were obtained with a Radiance 2000 (Bio-Rad) confocal microscope.

Murine P- and E-selectin and TNF blockade. mAbs against murine P-selectin (5H1, rat IgG1; 50 μg/mouse) and E-selectin (9A9, rat IgG2b; 50 μg/mouse), etanercept (TNF blocker, 5 mg/kg body weight; Amgen), or irrelevant control mAbs were injected intraperitoneally twice a week for 2 weeks, starting at 1 week of age. Mice were killed 3 days after the final injection.

Tn antigen expression in UC patients. The UC patient sample study was approved by the Institutional Review Boards of the Oklahoma Medical Research Foundation and the University of Oklahoma Health Science Center. De-identified, archived paraffin sections of human UC colon biopsy samples were first stained for expression of Tn antigens using anti-Tn antigen. Deparaffinized sections were incubated with biotinylated mAb against Tn (mouse IgM), after streptavidin/biotin and nonspecific protein blocking. The sections were then incubated with HRP-streptavidin (Vector Laboratories) for 30 minutes, and then developed with a DAB kit (Vector Laboratories) and counterstained with hematoxylin.

Statistics. All data are presented as the mean ± SEM, unless otherwise indicated. Unpaired 2-tailed Student's *t* test was used to analyze the difference between 2 groups. A *P* value less than 0.05 was considered to be significant.

Acknowledgments

We thank Rodger McEver for helpful discussions and critical review of the manuscript. We thank Shizuo Akira for providing TLR4- and Myd88-deficient mice and Sylvie Robine and Robert

Coffey for VillinCre-ER^{T2} transgenic mice. The anti-Tn was provided by Richard Cummings and Tongzhong Ju. We thank Ling Chen and Randy May for technical support. Laser capture microdissection was carried out in the advanced immunohistochemistry and morphology core facility of the Department of Medicine, Digestive Diseases, and Nutrition, University of Oklahoma Health Sciences Center. Tissue processing was performed in the imaging core facility of the Oklahoma Medical Research Foundation. This work was supported by NIH grants RR018758 (to L. Xia) and R01DK085691 (to L. Xia); by a Senior Research Award (to L. Xia) from the Crohn's and Colitis Foundation of America; and by the Swedish Research Council (7461, 21027, and 342-2004-4434 to G.C. Hansson), Torsten och Ragnar Söderbergs Stiftelser (to G.C. Hansson), and The Swedish Foundation for Strategic Research — Innate Immunity Program (to G.C. Hansson).

Received for publication October 25, 2010, and accepted in revised form January 12, 2011.

Address correspondence to: Lijun Xia, Cardiovascular Biology Research Program, Oklahoma Medical Research Foundation, 825 N.E. 13th Street, Oklahoma City, Oklahoma 73104, USA. Phone: 405.271.7892; Fax: 405.271.3137; E-mail: lijun-Xia@omrf.org.

Xiaowei Liu's present address is: Second Xiangya Hospital, Central South University, Changsha, Hunan, China.

1. Xavier RJ, Podolsky DK. Unravelling the pathogenesis of inflammatory bowel disease. *Nature*. 2007;448(7152):427–434.
2. Abraham C, Cho JH. Inflammatory bowel disease. *N Engl J Med*. 2009;361(21):2066–2078.
3. Garrett WS, Gordon JI, Glimcher LH. Homeostasis and inflammation in the intestine. *Cell*. 2010;140(6):859–870.
4. Johansson ME, Holmén Larsson JM, Hansson GC. Microbes and Health Sackler Colloquium: The two mucus layers of colon are organized by the MUC2 mucin, whereas the outer layer is a legislator of host-microbial interactions. [published online ahead of print June 25, 2010]. *Proc Natl Acad Sci U S A*. doi:10.1073/pnas.1006451107.
5. Ponda PP, Mayer L. Mucosal epithelium in health and disease. *Curr Mol Med*. 2005;5(6):549–556.
6. Zaph C, et al. Epithelial-cell-intrinsic IKK-beta expression regulates intestinal immune homeostasis. *Nature*. 2007;446(7135):552–556.
7. Olson TS, et al. The primary defect in experimental ileitis originates from a nonhematopoietic source. *J Exp Med*. 2006;203(3):541–552.
8. Johansson ME, Phillipson M, Petersson J, Velcich A, Holm L, Hansson GC. The inner of the two Muc2 mucin-dependent mucus layers in colon is devoid of bacteria. *Proc Natl Acad Sci U S A*. 2008; 105(39):15064–15069.
9. Gum JR Jr, Hicks JW, Toribara NW, Siddiki B, Kim YS. Molecular cloning of human intestinal mucin (MUC2) cDNA. Identification of the amino terminus and overall sequence similarity to prepro-von Willebrand factor. *J Biol Chem*. 1994;269(4):2440–2446.
10. Ju T, Brewer K, D'Souza A, Cummings RD, Canfield WM. Cloning and expression of human core 1 beta1,3-galactosyltransferase. *J Biol Chem*. 2002; 277(1):178–186.
11. Fu J, et al. Endothelial cell O-glycan deficiency causes blood/lymphatic misconnections and consequent fatty liver disease in mice. *J Clin Invest*. 2008;118(11):3725–3737.
12. Xia L, et al. Defective angiogenesis and fatal embryonic hemorrhage in mice lacking core 1-derived O-glycans. *J Cell Biol*. 2004;164(3):451–459.
13. Ju T, Aryal RP, Stowell CJ, Cummings RD. Regulation of protein O-glycosylation by the endoplasmic reticulum-localized molecular chaperone Cosmc. *J Cell Biol*. 2008;182(3):531–542.
14. Smithson JE, Campbell A, Andrews JM, Milton JD, Pigott R, Jewell DP. Altered expression of mucins throughout the colon in ulcerative colitis. *Gut*. 1997;40(2):234–240.
15. Podolsky DK, Isselbacher KJ. Composition of human colonic mucin. Selective alteration in inflammatory bowel disease. *J Clin Invest*. 1983;72(1):142–153.
16. Rhodes JM. Colonic mucus and ulcerative colitis. *Gut*. 1997;40(6):807–808.
17. Corfield AP, et al. Colonic mucins in ulcerative colitis: evidence for loss of sulfation. *Glycoconj J*. 1996;13(5):809–822.
18. Podolsky DK, Fournier DA. Alterations in mucosal content of colonic glycoconjugates in inflammatory bowel disease defined by monoclonal antibodies. *Gastroenterology*. 1988;95(2):379–387.
19. Madison BB, Dunbar L, Qiao XT, Braunstein K, Braunstein E, Gumucio DL. Cis elements of the villin gene control expression in restricted domains of the vertical (crypt) and horizontal (duodenum, cecum) axes of the intestine. *J Biol Chem*. 2002; 277(36):33275–33283.
20. Elson CO, Cong Y, McCracken VJ, Dimmitt RA, Lorenz RG, Weaver CT. Experimental models of inflammatory bowel disease reveal innate, adaptive, and regulatory mechanisms of host dialogue with the microbiota. *Immunol Rev*. 2005;206:260–276.
21. Mombaerts P, Iacomini J, Johnson RS, Herrup K, Tonegawa S, Papaioannou VE. RAG-1-deficient mice have no mature B and T lymphocytes. *Cell*. 1992; 68(5):869–877.
22. McEver RP. Adhesive interactions of leukocytes, platelets, and the vessel wall during hemostasis and inflammation. *Thromb Haemost*. 2001;86(3):746–756.
23. An G, et al. Increased susceptibility to colitis and colorectal tumors in mice lacking core 3-derived O-glycans. *J Exp Med*. 2007;204(6):1417–1429.
24. el Marjou F, et al. Tissue-specific and inducible Cre-mediated recombination in the gut epithelium. *Genesis*. 2004;39(3):186–193.
25. Marchiando AM, et al. Caveolin-1-dependent occludin endocytosis is required for TNF-induced tight junction regulation in vivo. *J Cell Biol*. 2010; 189(1):111–126.
26. Kaser A, et al. XBP1 links ER stress to intestinal inflammation and confers genetic risk for human inflammatory bowel disease. *Cell*. 2008; 134(5):743–756.
27. Kornfeld R, Kornfeld S. Assembly of asparagine-linked oligosaccharides. *Annu Rev Biochem*. 1985; 54:631–664.
28. Tarp MA, Clausen H. Mucin-type O-glycosylation and its potential use in drug and vaccine development. *Biochim Biophys Acta*. 2008;1780(3):546–563.
29. Samali A, Fitzgerald U, Deegan S, Gupta S. Methods for monitoring endoplasmic reticulum stress and the unfolded protein response. [published online ahead of print October 12, 2009]. *Int J Cell Biol*. doi:10.1155/2010/83037.
30. Ju T, Cummings RD. Protein glycosylation: chaperone mutation in Tn syndrome. *Nature*. 2005; 437(7063):1252.
31. Ju T, et al. Human tumor antigens Tn and sialyl Tn arise from mutations in Cosmc. *Cancer Res*. 2008; 68(6):1636–1646.
32. Corfield AP, Carroll D, Myerscough N, Probert CS. Mucins in the gastrointestinal tract in health and disease. *Front Biosci*. 2001;6:D1321–D1357.
33. Van Klinken BJ, Van der Wal JW, Einerhand AW, Buller HA, Dekker J. Sulphation and secretion of the predominant secretory human colonic mucin MUC2 in ulcerative colitis. *Gut*. 1999;44(3):387–393.
34. Van der Sluis M, et al. Muc2-deficient mice spontaneously develop colitis, indicating that MUC2 is critical for colonic protection. *Gastroenterology*. 2006; 131(1):117–129.
35. Heazlewood CK, et al. Aberrant mucin assembly in mice causes endoplasmic reticulum stress and spontaneous inflammation resembling ulcerative colitis. *PLoS Med*. 2008;5(3):e54.
36. Johansson ME, et al. Bacteria penetrate the inner mucus layer before inflammation in the dextran sulfate colitis model. *PLoS One*. 2010;5(8):e12238.
37. Bergstrom KS, et al. Muc2 protects against lethal infectious colitis by disassociating pathogenic and commensal bacteria from the colonic mucosa. *PLoS Pathog*. 2010;6(5):e1000902.
38. Hasnain SZ, et al. Mucin gene deficiency in mice impairs host resistance to an enteric parasitic infection. *Gastroenterology*. 2010;138(5):1763–1771.
39. Shirazi T, Longman RJ, Corfield AP, Probert CS. Mucins and inflammatory bowel disease. *Postgrad Med J*. 2000;76(898):473–478.
40. Prescott NJ, et al. A nonsynonymous SNP in ATG16L1 predisposes to ileal Crohn's disease and is independent of CARD15 and IBD5. *Gastroenterology*. 2007;132(5):1665–1671.
41. McGovern DP, et al. Fucosyltransferase 2 (FUT2) non-secretor status is associated with Crohn's disease. *Hum Mol Genet*. 2010;19(17):3468–3476.
42. Varki A, et al. *Essentials of Glycobiology*. Cold Spring Harbor, New York, USA: Cold Spring Harbor Press; 2009.
43. Strober W, Fuss I, Mannon P. The fundamental basis of inflammatory bowel disease. *J Clin Invest*. 2007;117(3):514–521.
44. Garrett WS, et al. Communicable ulcerative colitis induced by T-bet deficiency in the innate immune system. *Cell*. 2007;131(1):33–45.
45. Martens EC, Chiang HC, Gordon JI. Mucosal glycan foraging enhances fitness and transmission of a saccharolytic human gut bacterial symbiont. *Cell Host Microbe*. 2008;4(5):447–457.
46. Strober W, Fuss IJ, Blumberg RS. The immunology of mucosal models of inflammation. *Annu Rev Immunol*. 2002;20:495–549.
47. Williams SA, Xia L, Cummings RD, McEver RP, Stanley P. Fertilization in mouse does not require terminal galactose or N-acetylglucosamine on the zona pellucida glycans. *J Cell Sci*. 2007;120(pt 8):1341–1349.
48. Akira S, Uematsu S, Takeuchi O. Pathogen recognition and innate immunity. *Cell*. 2006;124(4):783–801.
49. Rakoff-Nahoum S, Paglino J, Eslami-Varzaneh F, Edberg S, Medzhitov R. Recognition of commensal microflora by toll-like receptors is required for intestinal homeostasis. *Cell*. 2004;118(2):229–241.